Journal of Chromatography A, 1217 (2010) 1298–1304

Contents lists available at ScienceDirect

Journal of Chromatography A

journal homepage: www.elsevier.com/locate/chroma

Preparation and characterization of novel macroporous cellulose beads regenerated from ionic liquid for fast chromatography

Kai-Feng Du[a], Min Yan[b], Quan-Yi Wang[a], Hang Song[a,*]

[a] Department of Pharmaceutical & Biological Engineering, School of Chemical Engineering, Sichuan University, Chengdu 610065, China
[b] Department of Computer, Sichuan TOP Vocational Institute of Information Technology, Chengdu 611743, China

ARTICLE INFO

Article history:
Received 27 May 2009
Received in revised form
11 December 2009
Accepted 15 December 2009
Available online 22 December 2009

Keywords:
Macroporous cellulose beads
Ionic liquid
Permeability
Dynamic binding capacity
Column efficiency
Fast chromatography

ABSTRACT

Macroporous cellulose beads (MCB) used as anion exchangers were successfully prepared from cellulose solution in ionic liquid by double emulsification followed by cross-linking and modification with diethylaminoethyl. The pore structure and properties of the MCB were investigated and the results were compared with homogeneous cellulose beads (HCB). The MCB in size of about 71 μm is characterized by two sets of pores, i.e., diffusion pores (10–20 nm) and macropores (800–2000 nm), determined by mercury porosimeter. In addition, the bed permeability and effective porosity for BSA of MCB-packed column are 58% and 25% higher than those of HCB-packed column, respectively. The adsorption properties of MCB were evaluated, and compared with HCB and commercial absorbent (Sepharose 6 Fast Flow, CSFF). It is found that the pore diffusivity of BSA in MCB is over 7.9 times higher than HCB, and 6.7 times higher than CSFF, respectively. While the equilibrium adsorption capacity (q_m) of BSA on MCB is obviously lower than that on HCB and CSFF, the dynamic binding capacity (DBC) on MCB at 10% breakthrough reaches 47.7 mg/mL, higher than HCB (40.3 mg/mL) and CSFF (46.2 mg/mL) at flow rate of 360 cm/h. In addition, the MCB-packed column showed better column efficiency over the HCB packed one. Therefore, we demonstrated that the MCB possessed more advantages than other ones, like HCB and CSFF, and was expected as an ideal material for fast chromatography.

1. Introduction

Liquid chromatography (LC) is a useful and popular technique that can provide a high degree of resolution for a wide range of bioseparation. As for this technique, the stationary phase is the key element that relates significantly to the chromatographic performance [1–4]. In this context, growing efforts have been directed to fabricate a novel stationary phase that can satisfy a specific separation need.

The particular performance of liquid chromatography is determined mainly by the structural constitution of stationary phase, indicating its size and pore distribution [2,5], because percolation of the mobile phase through stationary phase is an essential feature during the chromatographic process. Hence, modifying the pore structure of stationary phases is an efficient way to improve the chromatography performance. In the subject of structure design of stationary phase, a kind of bimodal pore adsorbent has been developed and used in fast separation of biological molecules. The novel material is characterized by both macropores and diffusive pores, and can be expected to show superior adsorption properties during the chromatography process. Firstly, the interconnected macropores provide more wide channels through the absorbent for convective flow of the mobile phase, thus effectively increase mass transfer. Secondly, the diffusive pores, connecting the macropores, expose more amounts of adsorption sites for a high absorption capacity of large molecules. These properties are especially suitable for purifying biological molecules in a fast chromatography. Until now, numerous bimodal pore beads made of agarose [3], polystyrene [6] and methacrylates [7] have been fabricated and widely used for the separation of biological molecules.

Cellulose is a kind of linear polysaccharide, and widely used as the chromatographic support for purifying biological molecules [8,9]. The popularity lies in that cellulose exhibits biocompatibility to biological molecules, ease modification with usual ligands, and suitable porosity for high adsorption capacity [8–11]. Despite many advantages, the synthetic rotes to cellulose-based supports, especially bimodal pore beads, are less common. The major obstacle can be ascribed to that cellulose is insoluble in water and common organic solvent because of its well developed intermolecular hydrogen bonding [12]. Until now, only a limited number of solvent systems for dissolving cellulose have been found, such as N-methylmorpholine N-oxide monohydrate (NMMO), LiCl/N,N-dimethylacetamide (DMAc), ammonium fluorides/dimethylsulfoxide, as well as molten salt hydrates[12,13].

* Corresponding author. Tel.: +86 28 85405221; fax: +86 28 85405221.
E-mail address: hangsong@vip.sina.com (H. Song).

0021-9673/$ – see front matter © 2009 Elsevier B.V. All rights reserved.
doi:10.1016/j.chroma.2009.12.037

However, these solvents are some environmentally unacceptable. Among these solvents, only NMMO is used on the industrial scale for cellulose processing. However, NMMO also possesses some disadvantages, such as thermal instability, side reaction, and high temperature for the dissolution process [12]. Hence, there is still a strong demand for new solvents for cellulose processing.

Very recently, various ionic liquids, so called green solvents, were encouraged to find to dissolve cellulose as well. In 2002, Rogers and co-workers firstly reported that that cellulose could be dissolved in ionic liquid (1-butyl-3-methylimidazolium chloride, IL), and investigated its dissolution properties [14]. In the following years, further studies on IL for dissolving cellulose have been carried out, and successfully prepared several cellulose materials, like fiber, film, and gel [12,15–17]. Compared with other common solvents, the IL possesses several advantages, such as lack of any measurable vapor pressure, ease of recycling, high thermal stability, and ease to operate [12,14]. Given these properties, the advent of novel solvent would make it process a bright future for cellulose-based materials.

Inspired by the new progress in cellulose solvent [12,14], in the present work, we have attempted to fabricate cellulose beads with macropores for fast protein chromatography by a method that combined double emulsification procedure and cellulose regeneration from ionic liquid. Mechanical strength of the porous cellulose beads was further enhanced by a cross-linking reaction. Furthermore, derivatized with diethylaminoethyl groups, the anion macroporous cellulose beads were prepared, and compared them with homogeneous ones and commercial absorbents (Sepharose 6 Fast Flow). For comparison, the physical and chromatographic properties of the absorbents, such as morphology, pore size distribution, flow hydrodynamics, adsorption behavior, were investigated and discussed in detail to reveal the advantages of the macroporous cellulose beads for fast protein chromatography.

2. Experimental

2.1. Materials

Microcrystalline cellulose was provided from Shanhe Medicinal Accessary Material (Anhui, China). 1-Butyl-3-methylimidazolium chloride (ionic liquid, IL) was purchased from TCI (Shanghai, China). Polyethylene glycol sorbitan monostearate (Tween 60) and sorbitan trioleate (Span 85) were obtained from Runhua (Guangdong, China). Tris(hydroxymethyl) aminomethane (Tris), diethylaminoethyl chloride (DEAE-Cl) and bovine serum albumin (BSA) were obtained from Sigma (MO, USA). Commercial Sepharose 6 Fast Flow (denoted as CSFF) was obtained from GE Biosciences (Uppsala, Sweden). Other regents, including transformer oil, glycol diglycidyl ether, epichlorohydrin and cyclohexane, were of analytical grade from local source.

2.2. Preparation of cellulose solution using ionic liquid as solvent

The cellulose solution of 7 wt% was manufactured using ionic liquid, 1-butyl-3-methylimidazolium chloride as dissolving solvent. Briefly, 10 g of anhydrous microcrystalline cellulose was submerged in 133 g of ionic liquid with magnetic stirring and heated for 13 h at 90 °C in oil bath. Finally, a clear, colorless, viscous cellulose solution was obtained and kept for the preparation of porous cellulose beads.

2.3. Preparation of porous cellulose beads

The macroporous cellulose beads were prepared using an improved double emulsification method. In the typical procedure, 20 mL of cellulose solution was added into a thermostatted stirred glass reactor containing 10 mL of cyclohexane and 0.8 mL of Tween 60 at 100 °C. After the mixture was emulsified by stirring at 2000 rpm for 10 min at 100 °C, the oil in water (O/W) emulsion of cellulose (emulsion I) was formed. Then, the disperse speed of stirrer was quickly down to 800 rpm and a thermostatted solution (100 °C) containing 80 mL of transformer oil and 3.6 mL of Span 85 was quickly poured into the emulsion I. After continually stirring for 10 min at 800 rpm, the O/W/O emulsion of cellulose (emulsion II) was formed. On the other hand, 100 mL of transformer oil containing 4.5 mL of Span 85 was emulsified with 40 mL of 0.2 mol/L aqueous sodium sulfate (Na_2SO_4) solution, which served as solidity solvent (emulsion III). Upon mixing the emulsion III with the emulsion II and lowering the temperature, the cellulose in emulsion II was precipitated from the ionic liquid solution through the regenerated hydrogen bonds between the cellulose fibers, and then formed the rigid cellulose beads. Subsequently, the rigid macroporous cellulose beads (denoted as MCB) were obtained by removal of the residual oil and ionic liquid using ethanol and distilled water. Moreover, homogeneous cellulose beads (denoted as HCB) were prepared without the preparation of emulsion I, as described in the above procedure. Before the further application, these beads were screened out with standard sieves of 200–300 meshes repeatedly until they showed relatively uniform size distribution by optical observation.

2.4. Double cross-linking and modification with DEAE-Cl

To enhance the mechanical strength, porous cellulose beads (MCB and HCB) were double cross-linked with glycol diglycidyl ether and epichlorohydrin as described by Pernemalm and Carlsson [18]. Briefly, 10 g of porous cellulose beads were mixed with 10 mL of glycol diglycidyl ether and stirred at 200 rpm for 40 min. Then, 20 mL of 3.0 mol/L NaOH solution was added and kept for 2.5 h at 40 °C. Subsequently, the first cross-linked porous cellulose beads were washed thoroughly with distilled water. Finally, these beads were further cross-linked using epichlorohydrin using the same procedure as described above. The cross-linked beads were then filtered and repeatedly washed with distilled water before modification.

The cross-linked MCB, HCB, and CSFF were derivatized with DEAE-Cl by the method of Shi et al. [19]. In the procedure, 10 mL of the absorbent was suspended in 20 mL of 2.0 mol/L DEAE-Cl solution and the mixture was heated to 60 °C in an incubator at 160 rpm for 10 min. Then, 20 mL of 3.5 mol/L NaOH was mixed with the suspension at 60 °C. After 1 h, the suspension was cooled down to room temperature and the formed anion absorbents were washed thoroughly by distilled water to neutralize pH. After the modification, the residual epoxide groups of the beads were reduced by reaction with 1 mol/L sulfuric acid [5].

2.5. Characterization of porous cellulose beads

The shapes and structures of customized cellulose beads were recorded by an XL 30 ESEM environmental scan electron microscope (Philips, Eindhoven, The Netherlands). In order to exhibit the real morphology of samples, the examples of cellulose beads (MCB and HCB) were transferred to 100% ethanol by first washing the beads with 20% ethanol and then gradually increasing the concentration of ethanol (10% increment, from 20% to 100%), and ethanol-dehydrated samples were carbon dioxide critical point dried in a model CPD-30 critical point dryer (BalTec, Balzers, Liechtenstein) before SEM. The particle size distribution and average size of wet cellulose beads were determined with a laser particle size analyzer, Mastersizer 2000 (Malvern Instruments, Malvern, UK). The intraparticle pore size distribution of the samples was determined by mercury porosimeter (Quantanchrome Corporation, USA). The surface areas of three dried absorbents were obtained

from N_2 adsorption measurement at −196 °C with a NOVA 2000 porosimeter (Quantachrome, USA). All chromatographic experiments were performed with Waters HPLC system (Waters, Milford, MA, USA) with a steel column of 100 mm × 4.6 mm i.d., companied with a model 600E multi-solvent delivery system, a Rheodyne 7725i injector valve (Rheodyne, Cotati, CA, USA) and a 2748 UV detector.

Hydrated density of wet samples was measured by water replacement in a pycnometer at atmosphere temperature [20]. The water content of beads was obtained by drying the samples in a vacuum thermostatic oven at 120 °C to a constant mass. The total ion exchange capacity of prepared samples was determined by a titration method [7].

The bed permeability (B_0) of MCB and HCB was calculated by the hydrodynamic data from the Darcy's law (1) [5].

$$\frac{\Delta p}{L} = \frac{u\mu}{B_0} \tag{1}$$

where Δp stands for pressure drop (Pa), L for column length (m), u for superficial velocity (m/s), μ for mobile phase viscosity (Pa s), B_0 for hydraulic permeability (m^2).

According to the Blake–Kozeny equation (2), the interparticle porosity (ε_b) can be obtained from the hydraulic permeability (B_0) and particle size (d_p) [21].

$$B_0 = \frac{d_p^2 \varepsilon_b^3}{150(1-\varepsilon_b)^2} \tag{2}$$

The effective porosity (ε_p) for protein was measured with BSA from the following Eq. (3) [22].

$$\varepsilon_p = \frac{V_e - V_{ex} - \varepsilon_b V_t}{(1-\varepsilon_b)V_t} \tag{3}$$

where V_e stands for the elution volume of BSA solution under non-retained condition, V_{ex} and V_t stand for the extra-column volume and total volume of column, respectively.

2.6. Protein adsorption equilibrium and kinetics

The equilibrium adsorption isotherms of DEAE-MCB, DEAE-HCB, and DEAE-CSFF for BSA were conducted by the finite batch adsorption experiments [22]. Briefly as follows, the absorbents were equilibrated with 10 mmol/L Tris–HCl buffer (pH 7.6) (Buffer A) and drained by a G3 sintered glass filter. Then, 0.1 g of the drained beads was added to a 10 mL BSA solution in the centrifuge tubes at varying initial concentrations. The centrifuge tubes were shaken in an incubator (170 rpm) at 25 °C for 24 h at to ensure equilibrium. Finally, the suspension was centrifuged and the BSA concentrations in supernatant were determined at 280 nm. The adsorbed capacity (q, mg/mL) of BSA was calculated by the following Eq. (4).

$$q = \frac{(c_0 - c)V\rho_w}{W} \tag{4}$$

where c_0 and c (mg/mL) stand for the initial and equilibrated concentration of BSA, respectively. V (mL) and W (g) stand for the solution volume and the weight of wet samples, respectively. ρ_w (g/mL) stands for the hydrated density of samples.

The Langmuir equation (5) was used to fit the experimental data to determine the isotherm parameters and equilibrium binding capacities (q_m) [5].

$$q = \frac{q_m c}{K_d + c} \tag{5}$$

where q_m and K_d stand for equilibrium binding capacity and dissociation constant, respectively.

The adsorption kinetics experiments for protein were carried out by the batchwise method [19]. Briefly as follows, 100 mL of 0.1 mg/mL BSA solution was mixed with 1.8 g of drained absorbent in a flask equipped with a magnetic stirrer (150 rpm) at 25 °C. Every 5 min, 2 mL of sample was periodically collected to determine BSA concentration, and then the sample was returned to the flask immediately. This procedure took less than 20 s. By this procedure, the BSA concentration drop in the bulk solution along with time was logged. The uptake kinetic data of BSA for the absorbents were simulated by a pore diffusion model, and then the effective pore diffusivities of BSA were determined.

The used pore diffusion model, based on the porous structure of spherical beads, begins with two assumptions. Firstly, the driving force for intraparticle mass transfer is protein concentration gradient in the pore phase. Secondly, the protein adsorbed to the available binding sites in the pore wall remains fixed, that is there is no surface diffusion. The governing continuity Eq. (6) for the intraparticle mass transfer by pore diffusion is described as follows [19].

$$\left(\varepsilon_p + \frac{dq}{dc_p}\right)\frac{\partial c_p}{\partial t} = -\frac{\varepsilon_p D_p}{r^2}\frac{\partial}{\partial r}\left(r^2\frac{\partial c_p}{\partial r}\right) \tag{6}$$

where D_p stands for the pore diffusivity. And, dq/dc_p represents the slope of adsorption isotherm expressed on a whole particle volume basis. The initial and boundary conditions are:

$$t = 0, \quad c_p = 0 \tag{6'}$$

$$r = 0, \quad \frac{\partial c_p}{\partial r} = 0 \tag{6''}$$

$$r = r_p, \quad c_p = c_b \tag{6'''}$$

In the model, the external mass transfer resistance is neglected, and the mass transfer of protein from the liquid phase to the solid phase is expressed as:

$$\frac{dc_b}{dt} = -\frac{3F}{r_p}\varepsilon_p D_p \left.\frac{\partial c_p}{\partial r}\right|_{r=r_p} \tag{7}$$

The initial condition for this equation for this equation is as follows:

$$t = 0, \quad c_b = c_{b,0} \tag{7'}$$

The model was applied to determine the diffusion coefficients of BSA on MCB, HCB, and CSFF by fitting protein uptake-time curves obtained from the kinetic adsorption experiments. Meanwhile, the above pore diffusion model was solved by the orthogonal collocation method with 20 orthogonal collection points along the adsorbent radius [23].

2.7. Chromatographic experiments

Frontal analysis experiments were carried out in buffer A to determine the breakthrough behavior of column packed with MCB, HCB, and CSFF, respectively. Firstly, after equilibration of the packed column in buffer A, 2 mg/mL BSA in buffer A was pumped into the column at a defined flow rate and the outlet absorbance of the effluent at 280 nm was monitored. After adsorption, the packed column was eluted using buffer A plus 1.0 mol/L NaCl (pH 7.6) (noted as buffer B). The dynamic binding capacity (DBC) was calculated from the breakthrough curve using Eq. (8) [5].

$$q_{10\%} = \frac{c_0 u(t_{10\%} - t_0)}{(1-\varepsilon)V_t} \tag{8}$$

where $q_{10\%}$ stands for the DBC of absorbent at 10% breakthrough, c_0 for the feed BSA concentration, u for the volumetric flow rate, $t_{10\%}$ for the time at 10% breakthrough, and t_0 for the retention time under non-retained condition.

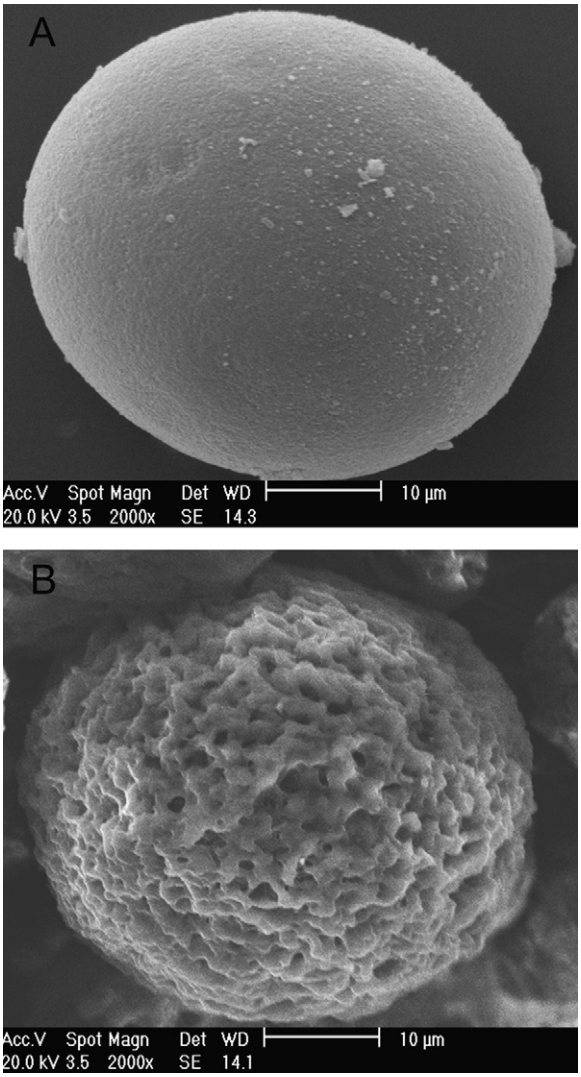

Fig. 1. SEM images of porous cellulose beads: (A) HCB and (B) MCB.

The column efficiency was expressed as the height of equivalent to a theoretical plate (HETP). It was measured by elution chromatography under the non-retained condition of BSA, and the data were analyzed by the moment analysis method to determine the HETP [5]. Typically, the column was equilibrated with 5 column volumes of buffer B, and 20 μL of 2 mg/mL BSA in buffer B was injected into the column and the outlet stream was recorded by UV detector at 280 nm. The dead volume of the system was measured by injecting acetone solution via the injection loop when chromatographic column was bypassed.

3. Results and discussion

3.1. Morphology and structure of porous cellulose beads

The porous cellulose beads were fabricated by an improved emulsification procedure and a double cross-linking reaction, as described in Section 2. Fig. 1 shows the SEM images of macroporous cellulose beads (MCB) and homogeneous cellulose beads (HCB), which were treated by critical point drying before SEM. It can be seen that all these dried beads have perfect spherical shape with size of about 45 μm, and there is a significant difference on the external morphology between MCB and HCB. From Fig. 1A, the HCB displays a smooth, homogeneous surface. In contrast, from Fig. 2B,

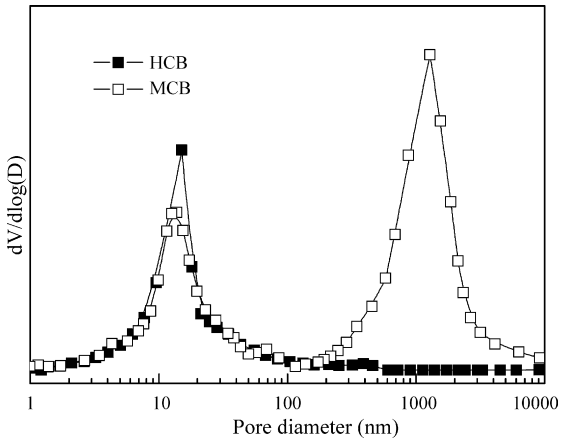

Fig. 2. Pore size distributions of porous cellulose beads: (■) HCB and (□) MCB.

the MCB is highly structured and exhibits a considerable number of interlaced wide-pores larger than 1 μm. Apparently, these large pores were originated from the removal of cyclohexane phase in the ionic liquid-cellulose phase. Similar results have been reports previously [24]. Furthermore, a similar cellulose adsorbent with wide-pore size of about 2.3 μm was prepared using $CaCO_3$ granules as templates, and the wide-pores in adsorbent were reduced to less than 1 μm after water removal from the observation of SEM images [25]. By the same token, the macropores would expand in size when the dried cellulose adsorbents are immerged into water. Therefore, it is expected that the expanded macropores in MCB are beneficial in reducing the mass transfer resistance and be favorable for fast protein purification.

The pore size of cellulose beads is an important index to evaluate the adsorbents, which strongly related to adsorption performance for protein. Mercury intrusion measurement is a popular method to obtain the pore size distribution of porous materials, including polysaccharide materials like agarose and cellulose beads [25,26]. Before mercury measurement, the cellulose beads were double cross-linked to enhance the structure stability. Moreover, the cross-linking treatment was necessary step to fabricate cellulose adsorbent and had no effect on the final pore size of cellulose beads. Fig. 2 represents the pore size distributions of the MCB and HCB. It is evident that the similar micropore size distributions (most range of 10–20 nm), denoted as diffusion pores, are characterized for both bead types and macropores (most range of 800–2000 nm) only for the MCB, which agrees well with the pore size estimated by the SEM image as shown in Fig. 1B. So, both diffusion pores and macropores in the MCB are identified. For further investigations, the surface areas were measured for MCB and HCB, as indicated in Table 1. As seen here, both beads appear to have similar surface area (35.5 m^2/g for MCB, 34.6 m^2/g for HCB), regardless of their significant difference in pore structure.

To order to clearly elucidate the physical properties of both MCB and HCB, more parameters were measured and listed in Table 1.

Table 1
Physical properties of HCB, MCB, and CSFF.

Matrix	HCB	MCB	CSFF
d_p (size range) (μm)	66 (37–108)	71 (40–112)	84 (50–131)
Surface area (m^2/g)	34.6	35.5	52.7
Hydrated density (g/mL)	1.15	1.08	1.03
Water content (%)	61	72	92
ε_p[a] (%)	48	60	55
B_0 ($\times 10^{-12}$ m^2)	3.33	5.26	–
ε_b	0.36	0.39	–

[a] Effective porosity for BSA.

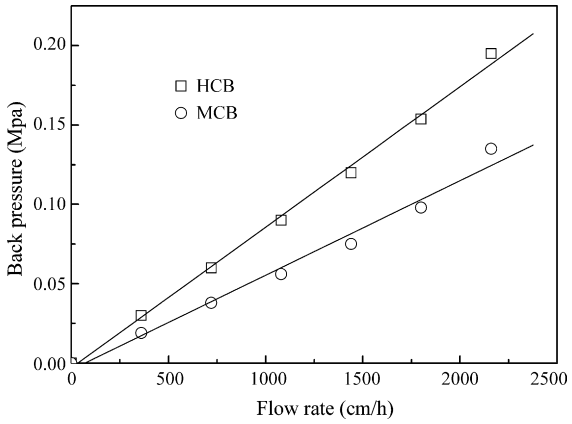

Fig. 3. Effect of flow rate on back pressure of the column packed with (□) HCB and (○) MCB. *Conditions*: column 100 mm × 4.6 mm i.d.; mobile phase, distilled water. The solid lines are calculated from Eq. (1).

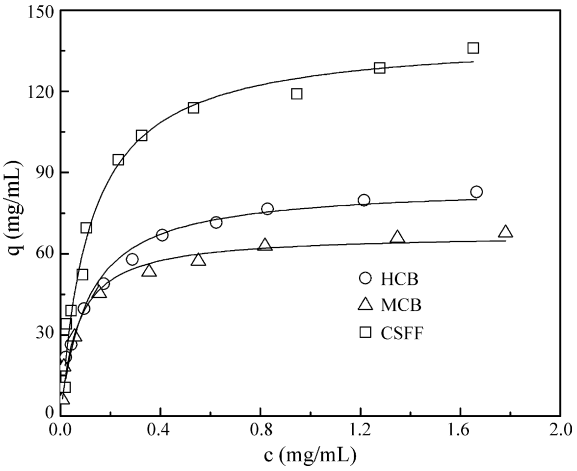

Fig. 4. Adsorption isotherms of BSA to the anion exchangers: (○) HCB; (△) MCB; (□) CSFF. The solid lines are calculated from Eq. (5).

It is clear that the volume-weighted mean diameter of wet MCB is about 71 μm (size range of 40–112 μm), and is similar to that of HCB (66 μm on average, size range of 37–108 μm), determined by particle size measurement. Given that the dried cellulose beads show about 45 μm in mean size from measurement of SEM, the swelling ratio is estimated to be nearly 56% in diameter. The MCB also exhibits a slightly lower hydrated density and higher water content than the HCB (Table 1). It is attributed to the partial substitution of cellulose gel by water in macropores within MCB. Moreover, these macroporous channels in MCB are readily accessible and amenable to the penetration of BSA into cellulose gel, so as to cause higher effective porosity (60%) of the MCB than that (48%) of the HCB for BSA.

One of the most significant properties of the cellulose beads on chromatography is their flow hydrodynamics in terms of the relationship between flow rate and back pressure. It strongly relates to the mechanical strength and mass transfer during the chromatographic process, which is mainly determined by the pore structure of the beads.

Fig. 3 shows the back pressure-flow rate curves for the columns packed with MCB and HCB under the same condition for comparison. As seen in Fig. 3, the curves are linear over the entire range of flow rates. It confirms that these cellulose beads were not compressed even at high flow rate up to over 2000 cm/h, indicating their excellent mechanical strength. With the flow rate increasing continually, while the backpressure-flow rate curve for MCB-packed column is still linear along with flow rate, the back pressure for HCB-packed column markedly increases and the linear relationship is destroyed (data not shown), indicating the HCB was compressed and not suitable for chromatography. This result demonstrates that the MCB has more extensive range of flow rate than the HCB during the chromatographic process. Moreover, in case of MCB, the column displays a lower back pressure compared with the HCB-packed column at a same flow rate. The lower back pressure of MCB might be ascribed to the introduction of macropores, which provides more wide channels for transporting mobile phase quickly through the cellulose gel.

To quantitatively evaluate the role of macropores in the MCB, the corresponding hydraulic permeability (B_0) and the interparticle porosity (ε_b) for both bead types were calculated from the hydraulic experiments and summarized in Table 1. It can be seen that the values of B_0 and ε_b for MCB-packed column is 58% and 8.3% higher than that for HCB-packed column, respectively. According to these results, introducing macropores in cellulose beads could decrease significantly the mass transfer resistance through the packed column, and then result in high permeability. With high permeability, the MCB would benefit the rapid purification of biological molecules in a fast chromatography.

3.2. Protein adsorption equilibrium and kinetics

The adsorption equilibrium of BSA on the anion absorbents was carried out by the finite batch adsorption experiment, being described in Section 2.6. Fig. 4 presents the results for equilibrium isotherms on MCB and HCB, and compared them with commercial Sepharose 6 Fast Flow (denoted as CSFF). Least-square fitting the isotherm data to Eq. (5) gave the equilibrium binding capacities (q_m) and dissociation constants (K_d) (Table 2). The results from Table 2 showed that the value of q_m for MCB reaches 67.2 mg/mL, 21.2% lower than that for HCB. The reduction of equilibrium binding capacity lies in that the high porosity and large pores of MCB result in less surface area for adsorption in this case, which in turn affects the adsorption capacity, as proved previously [5,19]. Meanwhile, compared with HCB, the total ion exchange capacity of DEAE-MCB decreased about 24.5%, quantitatively in agreement to the reduction degree for equilibrium binding capacity for BSA. However, for commercial adsorbent, CSFF appeared to have the largest equilibrium binding capacity (140.3 mg/mL), although ion exchange capacity of CSFF was lower than that of HCB. This is, of course, related to the high available surface area for binding protein in case of CSFF (Table 1).

The interconnected macroporous channels through the MCB are expected to play a major role in the protein adsorption by improving the mass transfer. To further illustrate the effect of macropores on the protein adsorption, the dynamic adsorption kinetics for the absorbents (MCB, HCB, and CSFF) were studied by the batchwise method. The adsorption data were then fitted using the pore diffusion model as described above, and the results are shown in Fig. 5. As seen here, the simulated results fit well to the experimen-

Table 2
Parameters of dynamic and static adsorption as well as kinetics for HCB, MCB, and CSFF.

Matrix	HCB	MCB	CSFF
Ion exchange capacity (μmol/mL)	124.1	99.6	119.7
q_m (mg/mL)	85.2 ± 2.6	67.2 ± 2.3	140.3 ± 2.2
K_d (mg/mL)	0.097 ± 0.014	0.068 ± 0.013	0.1172
D_p ($\times 10^{-12}$ m^2/s)	2.1	12.7	1.9
DBC[a] (mg/mL)	40.3	49.7	46.2

[a] Flow rate is 360 cm/h; the values of DBC on HCB, MCB, and CSFF are calculated at 10% breakthrough from the breakthrough curves.

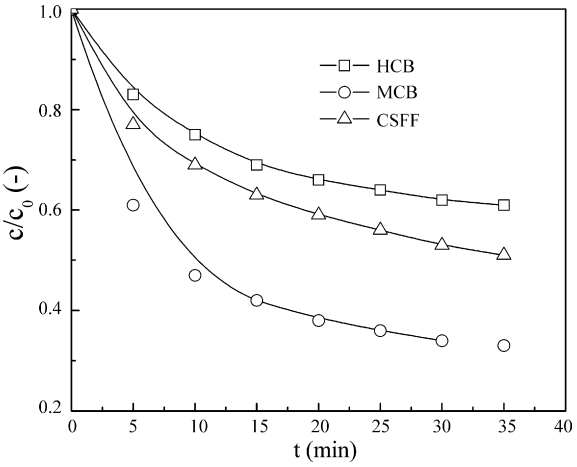

Fig. 5. Adsorption kinetic of BSA to the anion exchangers: (□) HCB; (○) MCB; (△) CSFF. The solid lines are calculated from Eq. (6).

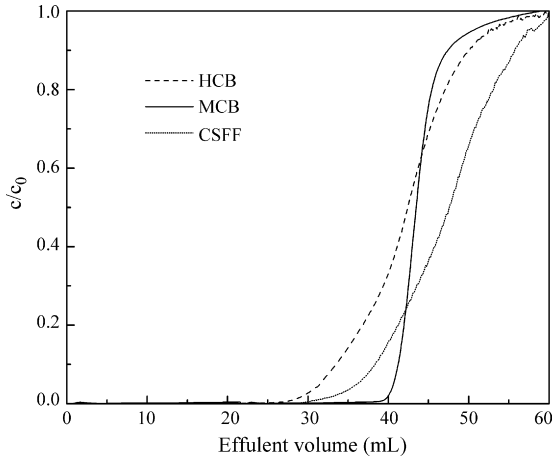

Fig. 6. Breakthrough curves of BSA for the anion exchangers: (- - -) HCB; (—) MCB; (···) CSFF.

tal data in the whole adsorption process, implying the model can explain protein adsorption on these beads satisfactorily. The corresponding effective pore diffusivity (D_p) of three beads types for BSA were extracted from the pore diffusion model and summarized in Table 2. Generally, the effective pore diffusivity (D_p) for proteins is related to the wide-pore size of adsorbents [25,26]. It can be seen that the D_p value of HCB is approaching to that of CSFF, suggests that both beads have similar adsorption kinetics for BSA, i.e., diffusional mass transfer. However, in case of MCB, the D_p value reaches 12.7×10^{-12} m^2/s, about 7.9 times higher than HCB, and 6.7 times higher than CSFF, respectively (Table 2). Meanwhile, Wang et al. reported a similar superporous adsorbent templated by granules. The new adsorbent showed a larger D_p value (3.91×10^{-12} m^2/s) over the homogenous ones and proved that the superpores benefited the mass transport for proteins, similar to our result. On the whole, the adsorption kinetics of protein is mainly controlled by pore structure through the adsorbent [23]. So, the improvements of adsorption kinetics can be explained by the fact that the macropores in MCB reduces the diffusion distance for protein transport, hence faster mass transfer performances.

3.3. Breakthrough behavior and dynamic binding capacity

Breakthrough experiment is another chromatographic technique for obtaining the pore-transport characteristics of the formed beads. The approach is more practical because of the more real reflection for the protein chromatographic process. Fig. 6 shows a series of breakthrough curves of BSA on MCB, HCB and CSFF at 360 cm/h of flow rate, respectively. The dynamic binding capacities (DBC) were calculated from Eq. (8) with the breakthrough curves, listed in Table 2. It is obvious that the breakthrough curve of MCB-packed column is very steeper in comparison with other two bead-packed columns. Moreover, the results from Table 2 show that the DBC of BSA on the absorbents is 49.7 mg/mL for MCB, 40.3 mg/mL for HCB, and 46.2 mg/mL for CSFF, respectively. The high DBC value on MCB indicates that more adsorption sites are available for absorbing protein in less time by introducing macropores in cellulose beads.

Fig. 7 shows the plots of DBC/q_m (dynamic-to-equilibrium binding capacity ratio) versus flow rate to MCB, HCB and CSFF, respectively. It can be observed from Fig. 7 that the DBC/q_m value is in the order of MCB > CSFF > HCB in the whole range of flow rate. Beyond that, the ratios of DBC/q_m on HCB and CSFF decline along with an increase of flow rate due to the slow protein diffusion into the absorbents. In contrast, for the example of MCB, the DBC/q_m value changes less than that of other absorbents (HCB and CSFF) in the tested flow rate. It suggests that the MCB can keep a high DBC even at an elevated flow rate. The comparison of MCB, HCB, and CSFF further confirms that the macropores in MCB weaken the mass transfer resistance, leading to more proteins available even at high flow rate. Hence, the value of DBC/q_m on MCB is higher and independent of flow rate. Taking into account the physical and chromatographic performances of the absorbent, MCB is considered to be promising for use in fast protein chromatography.

3.4. Column efficiency

Fig. 8 showed the relationship between column efficiency, described by HETP, and flow rate determined under the non-retained condition of BSA on the two beads types. At the lowest flow rate tested, i.e. 180 cm/h, the HETP of the HCB column is about 2.12 mm, 2.4 times larger than that of the MCB column (0.89 mm). With increasing flow rate, the HETP of the HCB column increases sharply, following a typical behavior expressed by the van Deemter equation. It indicates that the mass transfer resistance is significant in HCB. For the MCB column, however, the HETP increases less than that of the HCB column in the whole tested flow rates. The lower HETP values could be attributed to the present of macropores in MCB, which substantially reduced intraparticle mass transfer resistance. The similar results were reported in previous literatures [5,25]. Therefore, the macroporous cellulose beads, denoted

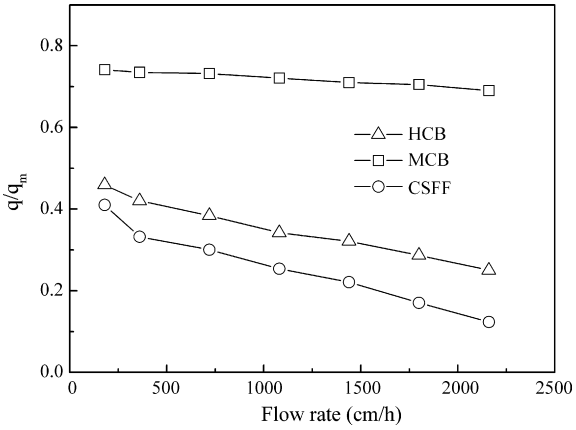

Fig. 7. Effect of flow rate on the DBC/q_m for the anion exchangers: (△) HCB; (□) MCB; (○) CSFF. The DBC of the exchangers are calculated at 10% breakthrough from Eq. (8).

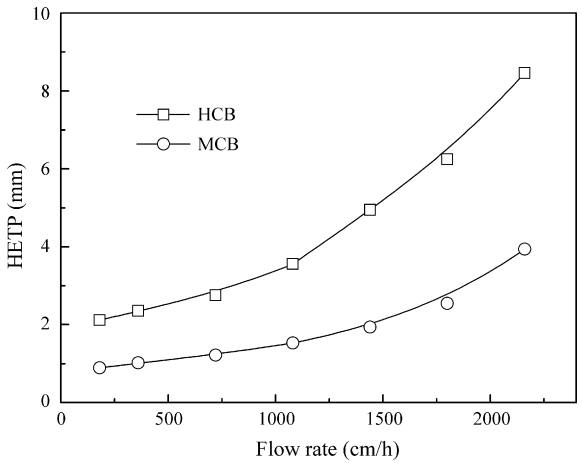

Fig. 8. Column efficiency detected with BSA as a function of flow rate: (□) HCB; (○) MCB.

as MCB, is considered to be promising for use in fast protein chromatography.

4. Conclusions

A novel route to prepare macroporous cellulose beads (MCB) has been successfully developed by a double emulsification process of cellulose solution in ionic liquid. The bimodal pore structure and corresponding properties were determined by means of different techniques including SEM, pore size distribution, particle size distribution, water contend measurement, flow hydrodynamics, adsorption kinetics, static and dynamic adsorption, as well as column efficiency. It is demonstrated that the generated cellulose beads possess two sets of pores, i.e., diffusion pores featured for all cellulose beads and macropores only for MCB. It is encouraging to see that introducing macropores in cellulose beads could enhance effectively bed permeability, improve significantly effective pore diffusivity and dynamic binding capacity for protein, and column efficiency. Beyond that, the absorbent of MCB also possesses some advantages, like permeability, dynamic binding capacity for protein, over commercial adsorbent (Sepharose 6 Flow fast, SCFF). All of the properties indicate the example of MCB is an ideal stationary phase for purifying biological molecules in fast chromatography. In addition, compared with other approaches to fabricate porous cellulose beads, the present strategy provides a novel readily, green procedure for the fabrication of cellulose-based beads.

Acknowledgment

This work was supported by Foundation of Sichuan University for Young Teachers.

References

[1] G. Guiochon, J. Chromatogr. A 1168 (2007) 101.
[2] M. Leonard, J. Chromatogr. B 699 (1997) 3.
[3] P.E. Gustavsson, P.O. Larsson, J. Chromatogr. A 734 (1996) 231.
[4] Y. Ding, Y. Sun, Chem. Eng. Sci. 60 (2005) 917.
[5] K.F. Du, D. Yang, Y. Sun, J. Chromatogr. A 1163 (2007) 212.
[6] J.B. Qu, W.Q. Zhou, W. Wei, Z.G. Su, G.H. Ma, Langmuir 24 (2008) 13646.
[7] G.Y. Sun, Q.H. Shi, Y. Sun, J. Chromatogr. A 1061 (2004) 159.
[8] H. Xia, D. Lin, S. Yao, J. Chromatogr. A 1175 (2007) 55.
[9] E. Ruckenstein, W. Guo, Biotechnol. Prog. 20 (2004) 13.
[10] W.D. Oliveira, W.G. Glasser, J. Appl. Polym. Sci. 60 (1996) 63.
[11] M. Kavoosi, D. Lam, J. Bryan, D.G. Kilburn, C.A. Haynes, J. Chromatogr. A 1175 (2007) 187.
[12] F. Hermanutz, F. Gahr, E. Uerdinger, F. Meister, B. Kosan, Macromol. Symp. 262 (2008) 23.
[13] T. Heinze, K. Schwikal, S. Barthel, Macromol. Biosci. 5 (2005) 520.
[14] R.P. Swatloski, S.K. Spear, J.D. Holbrey, R.D. Rogers, J. Am. Chem. Soc. 124 (2002) 4974.
[15] M.B. Turner, S.K. Spear, J.D. Holbrey, R.D. Rogers, Biomacromolecules 5 (2004) 1379.
[16] M. Bagheri, H. Rodríguez, R.P. Swatloski, S.K. Spear, D.T. Daly, R.D. Rogers, Biomacromolecules 9 (2008) 381.
[17] J.I. Kadokawa, M.A. Murakami, Y. Kaneko, Carbohyd. Res. 343 (2008) 769.
[18] P.A. Pernemalm, M. Carlsson, G. Lindgren, Eur. Pat. Appl. 84850215.9 (1984).
[19] Q.H. Shi, X. Zhou, Y. Sun, Biotechnol. Bioeng. 92 (2005) 643.
[20] K.F. Du, D. Yang, Y. Sun, Ind. Eng. Chem. Res. 48 (2009) 755.
[21] C. Martin, J. Coyne, G. Carta, J. Chromatogr. A 1069 (2005) 43.
[22] S.P. Zhang, Y. Sun, AIChE J. 48 (2002) 178.
[23] W.D. Chen, X.Y. Dong, Y. Sun, J. Chromatogr. A 962 (2002) 29.
[24] P. Tiainen, P.E. Gustavsson, A. Ljungöf, P.O. Larsson, J. Chromatogr. A 1138 (2007) 84.
[25] D.M. Wang, G. Hao, Q.H. Shi, Y. Sun, J. Chromatogr. A 1146 (2007) 32.
[26] X. Zhou, Y. Sun, Z. Liu, Biochem. Eng. J. 34 (2007) 99.